2

Electrical Transport in Ternary Alloys: AlGaN and InGaN and Their Role in Optoelectronic

N. Bachir, A. Hamdoune and N. E. Chabane Sari
University of Abou–Baker Belkaid,
Tlemcen /Unity of Research Materials and Renewable Energies,
Algeria

1. Introduction

Since 1997, the market availability of blue, green and amber light emitting diode (LEDs), allows us to hope in time, obtaining the full range of the visible spectrum with semiconductor devices. Indeed, the development of blue emitters is very important because the blue emission is the last missing for the reconstruction of white light. Components based on gallium nitride (GaN) are the most effective in this area. In view of their low energy consumption and their high reliability, their use for the roadside (traffic lights) and domestic lighting may supersede the use of conventional incandescent or fluorescent lamps. In addition; the possibility offered by nitrides and their alloys, because of their intrinsic properties to develop blue and ultraviolet lasers, allows the production of systems that have greater storage capacity and playback of digital information (densities above the gigabit per square centimeter): the capacity is multiplied by four.

Research on GaN began in the 60s and the first blue LED based on GaN was performed in 1971 (Pankov et al., 1971). The development of GaN has been limited by the poor quality of the material obtained, and the failures in attempts to doping p. Recent research has resulted in a material of good quality, and in the development of doping p. These two achievements have developed the LEDs and lasers based on nitrides.

GaN has a direct band gap, high chemical stability, very good mechanical and physical properties, allowing it to be attractive for both optoelectronic and electronic devices operating at high temperature, high power and high frequency.

The development of InGaN alloys also allowed competing with GaP to obtain green LEDs. Table 1 shows the performance of GaN-based LEDs, compared with those obtained by other materials.

Given the performance obtained with the nitrides, the industrialization of blue and green LEDs was then very fast and has preceded the understanding of physical phenomena involved in these materials. Today, one of the major objectives of basic research on III-nitrides, is to identify key parameters that govern the emission of light in nanostructures (quantum wells or quantum dots) used as active layers of electroluminescent devices.

	Material	Wavelength emission	Light intensity	Emitted power	External quantum efficiency
Red	GaAlAs	660nm	1790mCd	4855µW	12.83%
Green	GaP	555nm	63mCd	30µW	0.07%
Green	InGaN	500nm	2000mCd	1000µW	2.01%
Blue	SiC	470nm	9mCd	11µW	0.02%
Blue	InGaN	450nm	2500mCd	3000µW	11%

Table 1. Performance of LEDs based on GaN and other materials (Agnès, 1999).

The two recurring problems concern the polarization effects related to the hexagonal structure of these materials, and also the effects of localization of carriers in the alloys.

Despite the technological and businessical advanced of these devices, some basic parameters of these materials remain little. The difficulty of developing these materials and controling their electrical properties (doping control) has long limited the determination of their parameters and their use in electronic and optoelectronic components. Gallium nitride (GaN) does not exist in nature, so it must be deposited on another material (sapphire, silicon ...) that does not have the same structural properties. This disagreement affects the optical and electronic qualities of those materials. The optimization of the devices thus requires a thorough understanding of the basic parameters and physical effects that govern the optical and electronic properties of these semiconductors.

The binary and ternary compounds based on GaN, exist in two structures: hexagonal and cubic. This second phase is far more difficult to develop and metastable, but it would present better electronic and optoelectronic performance. For this reason, we study the two ternary compounds AlGaN and InGaN in their cubic phases.

2. Band energy structures of the three nitrides

2.1 Status of the three nitrides in the family of semiconductors

The nature and bandgap energy are fundamental data in optoelectronics because direct gap materials have very large oscillator strength and the light emission is usually at energy close to that of the gap. The vast majority of semiconductor energy gap are located in the visible or near infrared. The family of nitrides stands in the UV (Fig. 1). GaN, AlN, InN and their alloys, are semiconductors with remarkable properties. The most important is undoubtedly their direct band gap ranging from 1.9eV (InN) to 3.4eV (GaN) (Nakamura S. & Fasol G., 1997), and reaches 6.2eV for AlN (fig. 1). With the concepts of the band gap engineering, developed in the context of III-V traditional semiconductors, it is possible to completely cover the visible spectral range, and to reach the ultraviolet A (320-400nm) and B (280-320nm). This is complemented by the strong stability of GaN what is responsible of the industrial production of light emitting diodes (LEDs), blue and green high brightness, and laser diodes (LDs) emitting at 0.4 microns. This makes these nitrides, the materials of choice for LEDs and laser diodes.

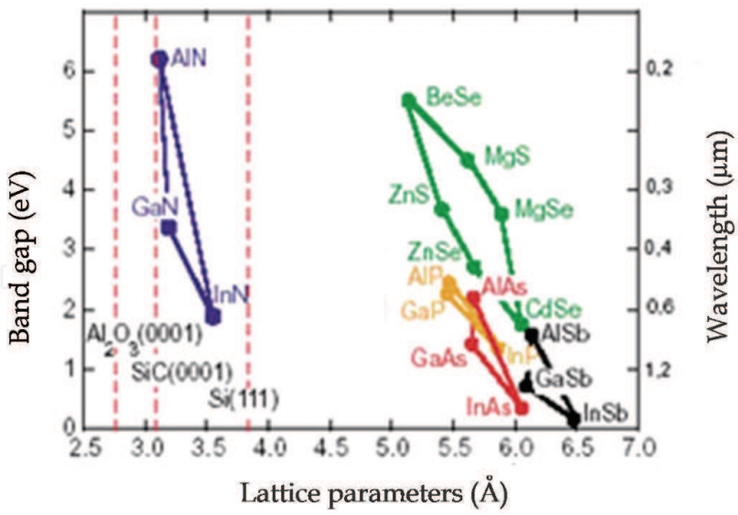

Fig. 1. Band gap and wavelength of various semiconductor compounds according to their lattice parameters (Nakamura & Fasol, 1997)

2.2 General forms of energy bands

The figure 2 shows the band structures in the cubic phase, of the gallium nitride (GaN), the aluminum nitride (AlN) and the indium nitride (InN).

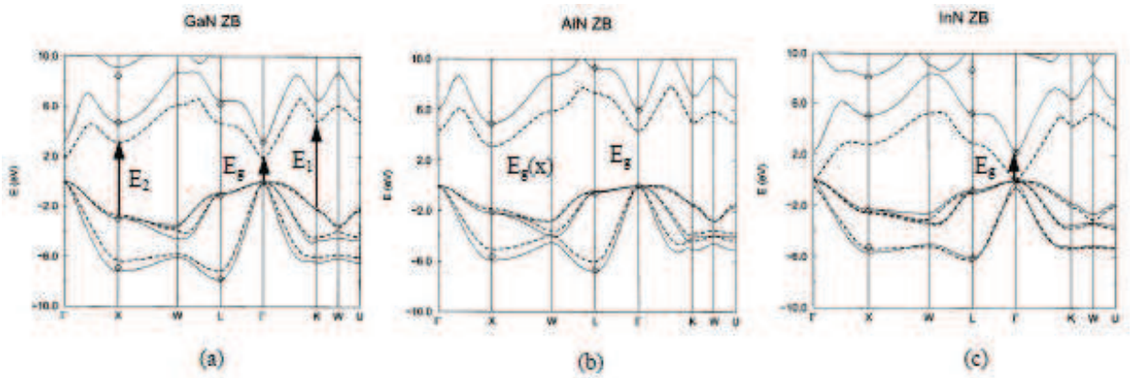

Fig. 2. Band structures of GaN, AlN, and InN in their cubic phases. The dotted lines correspond to results obtained by the "first-principles" method using VASP environment. The solid lines are those of the "semi-empirical pseudopotential" method (Martinez, 2002)

- Cubic GaN: In addition to the Γ valley, there are the L valley in the <111> direction and the X valley in the <100> direction, edge of the Brillouin zone. These last two valleys are characterized by a curvature smaller than that of the Γ valley and therefore the effective mass of electrons is higher and their mobility is lower. The minima of these valleys from the Γ band, are respectively about 2.6eV and 1.3eV (Martinez, 2002); they and are very large compared to other conventional III-V compounds.
- Cubic AlN: There are two minima between the conduction band and the valence band. However, the band structure shows a direct transition between points Γ corresponding to the gap.

- Cubic InN: The two minima between the conduction band and the valence band, have a very small difference, the gap in this case is very low.

2.3 Band-gaps (Nevou, 2008)

The first measurements of the band gap of GaN at low temperature date from the 1970s (Dingle et al., 1971). They gave a value of about 3.5eV at low temperatures. At room temperature, the band gap is about 3.39eV. Since the bandgap nitrides has been the subject of many studies (Davydov et al., 2002). The width of the band gap of AlN is of very short wavelengths that correspond to the near ultraviolet and far ultraviolet. At 300K, the energy gap is about 6.20eV, corresponding to a wavelength of 200nm. At 2K, the band gap is about 6.28eV (Vurgaftman & Meyer, 2003). The temperature dependence of the band gap is described by equation (1) of Varshni (Nakamura & Fasol, 1997):

$$Eg(T) = Eg(0) - \frac{\alpha \times T^2}{T + \beta} \tag{1}$$

Where Eg(0) is the bandgap at zero temperature, α and β are constants determined experimentally (Table 2).

material		Eg à 0K (eV)	Eg à 300K (eV)	α (eV/K)	β (K)
GaN	Cubic	3.28 (Bougrov et al., 2001)	3.2 (Bougrov et al., 2001)	0.593(Vurgaftman et al., 2001)	600(Vurgaftman et al., 2001)
	Hexagonal	3.51(Enjalbert, 2004)	3.43(Bethoux, 2004)	0,909 (Enjalbert, 2004)	830 (Enjalbert, 2004)
AlN	Cubic	6(Vurgaftman et al., 2001)	5.94(Dessene, 1998)	0.593(Vurgaftman et al., 2001)	600(Vurgaftman et al., 2001)
	Hexagonal	6.25(Enjalbert, 2004)	6.2 (Bethoux, 2004)	1.799 (Enjalbert, 2004)	1462(Enjalbert, 2004)
InN	Cubic	0.69 (Languy , 2007)	0.64 (Languy, 2007)	0.41 (Languy, 2007)	454 (Languy, 2007)
	Hexagonal	0.78(Enjalbert, 2004), 1.89(Anceau, 2004)	0.80(Bethoux, 2004), (Helman, 2004).	0.245 (Enjalbert, 2004)	624(Enjalbert, 2004)

Table 2. The energy gap at T = 0K and the parameters α and β, of the three nitrides in both phases.

The width of the band gap depends on the constraints applied to the material. For GaN, the biaxial compressive stress results in an increase in bandgap energy that is roughly linear with the applied stress. Since the lattice parameter "a" from the AlN is smaller than that of GaN (Fig. 3), the layers of the latter are in biaxial compression in the AlGaN alloy, resulting in increased energy band gap ~3,46–3,48eV (Martinez, 2002) at room temperature. As a result, the discontinuity of conduction band potential between GaN and AlN is reduced.

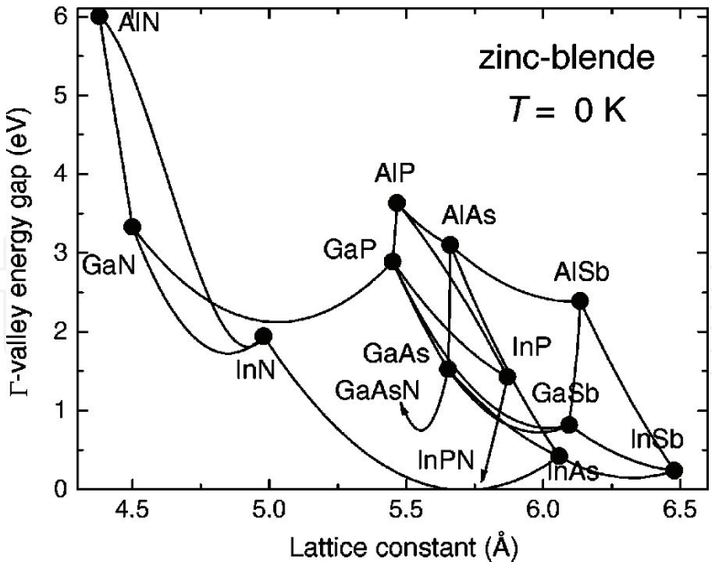

Fig. 3. The energy gap as a function of the lattice constant, for different cubic compounds at T = 0K (Vurgaftman et al., 2001).

2.3.1 The variation of AlxGa1-xN gap versus the x (Al) mole fraction

As a first approximation, the lattice parameters of AlxGa1-xN (InxGa1-xN) can be deduced from those of GaN and AlN (GaN and InN) by Vegard's law (Martinez, 2002) is a linear interpolation given by equation (2).

$$a_{Al_xGa_{1-x}N} = x \times a_{AlN} + (1-x) \times a_{GaN} \tag{2}$$

Moreover, the variation of the bandgap energy of the alloy according to the composition is not linear but quadratic; it is given by equation (3).

$$Eg(x) = x \times Eg(AlN) + (1-x) \times Eg(GaN) - bx \times (1-x) \tag{3}$$

The bowing parameter "b" is usually taken equal to 1.

Substituting Eg(AlN) and Eg(GaN) by their values at 300K in the relationship (3), we find the equations (4) and (5) which give the gaps respectively of cubic and hexagonal AlxGa1-xN, , according to x (Vurgaftman and Meyer, 2003):

$$Eg_1(x) = x^2 + 1.74x + 3.2eV \tag{4}$$

$$Eg_2(x) = x^2 - 1.77x + 3.43eV \tag{5}$$

By increasing the mole fraction of aluminum, the top of the valence band at Γ point, moves down and the energy gap increases.

Using MATLAB, we calculate the variation of AlxGa1-xN gap as a function of aluminum mole fraction; that is illustred by Figure 4.

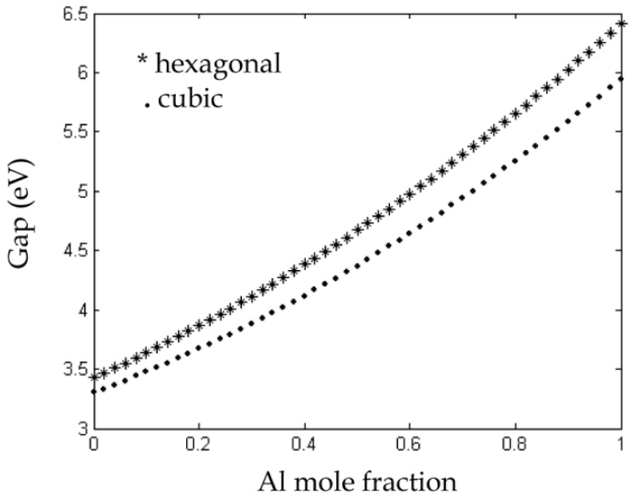

Fig. 4. Variation of AlxGa1-xN energy gap, versus the Al mole fraction (Castagné et al., 1989).

2.3.2 The variation of InxGa1-xN gap versus the x (In) mole fraction

To calculate the energy band gap, use the quadratic relationship (6) (JC Phillips):

$$Eg(InxGa1-xN) = x \times Eg(InN) + (1-x) \times Eg(GaN) - bx \times (1-x) \tag{6}$$

Substituting Eg(InN) and Eg(GaN) by their values at 300K, and taking b = 1, we find the equations (7) and (8) which give respectively gaps of cubic and hexagonal InxGa1-xN, as a function of x (Castagné et al., 1989):

$$Eg_1(x) = x^2 - 3.56x + 3.2eV \tag{7}$$

$$Eg_2(x) = x^2 - 3.63x + 3.43eV \tag{8}$$

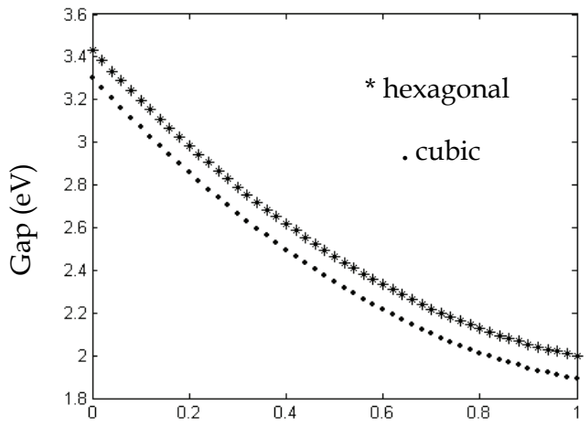

Fig. 5. Variation of $In_xGa_{1-x}N$ energy gap, versus the In mole fraction (Castagné et al., 1989).

The top of the valence band at Γ point shifts up and the energy gap decreases when the indium composition increases.

3. Electrical transport in ternary alloys: AlGaN and InGaN, and their role in optoelectronic

For zinc blend AlGaN and InGaN compounds, we calculate energy and velocity of the electrons for different mole fractions and various temperatures in the steady-state. We also calculate the electrons velocity in the transient mode.

We use Monte Carlo simulation method which is a program written in Fortran 90 MSDEV, and we simulate 20,000 electrons.

This method offers the possibility of reproducing the various microscopic phenomena residing in semiconductor materials. It is very important to study the transport properties of representative particles in the various layers of material over time; it is to follow the behavior of each electron subjected to an electric field in real space and in space of wave vectors. Indeed; over time, the electrons in the conduction band will have a behavior that results from the action of external electric field applied to them and their various interactions in the crystal lattice. We consider the dispersion of acoustic phonons, optical phonons, ionized impurities, intervalley and piezoelectric in a nonparabolic band.

Consider an electron which owns energy ε(t), wave-vector k (t), and which is placed in r (t). Under action of an applied electric field E (r, t); its interaction and exchange of energy with the lattice, and the deviation of its trajectory by impurities; this will modify its energy, its wave-vector and its position. Using the mechanic and the electrodynamics laws; we determine the behavior of each electron, in time and space. To be more realistic:

1. We statistically study possible energy exchanges between electrons, modes of lattice vibration and impurities; this allows us to calculate the probability of these interactions and their action on both electron energy and wave-vector.
2. We assume that these interactions are instantaneous. We can move electrons in free-flight under the only effect of electric field, between two shocks. The free-flight time is determined by the drawing of lots. When interaction takes place, we determine its nature by the drawing of lots. In this case, the electron energy and the electron wave-vector are modified. This results in a change of electrons distribution; we then calculate the electric field that results, at enough small time intervals, to assume it constant between two calculations (Enjalbert, 2004) – (Pugh et al., 1999)– (Zhang Y.et al., 2000).

We consider a simplified model of three isotropic and non parabolic bands. The wave-vector and energy of the electron are related by using the equation (9) (O'Learyet al., 2006*).

$$\frac{\hbar^2 k^2}{2m^*} = \varepsilon(1+\alpha\varepsilon) \tag{9}$$

Where m* is their effective mass in the Γ valley, ħk denotes the magnitude of the crystal momentum, ε represents the electron energy, and α is the nonparabolicity factor of the considered valley, given by equation (10) (O'Learyet al., 2006*).

$$\alpha = \frac{1}{Eg} \times \left(1 - \frac{m^*}{m_e}\right)^2 \tag{10}$$

Where m_e and Eg denote the free electron mass and the energy gap, respectively.

$m_e = 0.20m_0$ for GaN, $m_e = 0.32m_0$ for Al (Chuang et Al. 1996), and $m_e = 0.11m_0$ for InN (O'Learyet al., 2006).

The longitudinal v_l and transverse v_t, acoustic velocities (Castagné, 1989)–(Garro et Al. 2007)–(Anwar, 2001) are calculated by using equations (11) and (12) (where ρ is the density of material, and Cij are elastic constants):

$$v_l = \left(\frac{c_l}{\rho}\right)^{1/2} \tag{11}$$

$$v_t = \left(\frac{c_t}{\rho}\right)^{1/2} \tag{12}$$

The constants, c_l and c_t, are combinations of elastic constants, given by equations (13) and (14):

$$c_l = \frac{3 \times c_{11} + 2 \times c_{12} + 4 \times c_{44}}{5} \tag{13}$$

$$c_t = \frac{c_{11} - c_{12} + 3 \times c_{44}}{5} \tag{14}$$

3.1 Description of the simulation software

This software can perform two basic functions. The first is devoted to probability theory from the usual expressions, considering a model with isotropic and nonparabolic three valleys (Γ, L, X). The second role is to determine the instantaneous magnitudes defined on a set of electrons (energy, speed, position) by the "Self Scattering" procedure for which the free-flight times are distributed to each electron.

The results are highly dependent on many parameters that characterize the material and which, unfortunately, are often very poorly understood.

We developed the software by making it more friendly and simple users. The general procedure for running this software is composed of three essential steps that can be summarized as follows:

1. Reading the data file for the parameters of the used material, such as energy gap, effective masses, deformation potentials, coefficients of nonparabolicity, speed of sound, concentration of impurities, temperature of the network, applied electric fields, etc.. in a file.txt.
2. Running the software.
3. Delivery of output files: the values of interaction probabilities, speeds in different valleys, the energies...

The essence of our Monte Carlo simulation algorithm, used to simulate the electron transport within the semiconductors, AlxGa1-xN and InxGa1-xN, is given by the diagram of Fig. 6; where ∂t is the free-flight time of electrons, ε is their energy, λq(ε) is their total scattering rate, T_{total} is the simulation time.

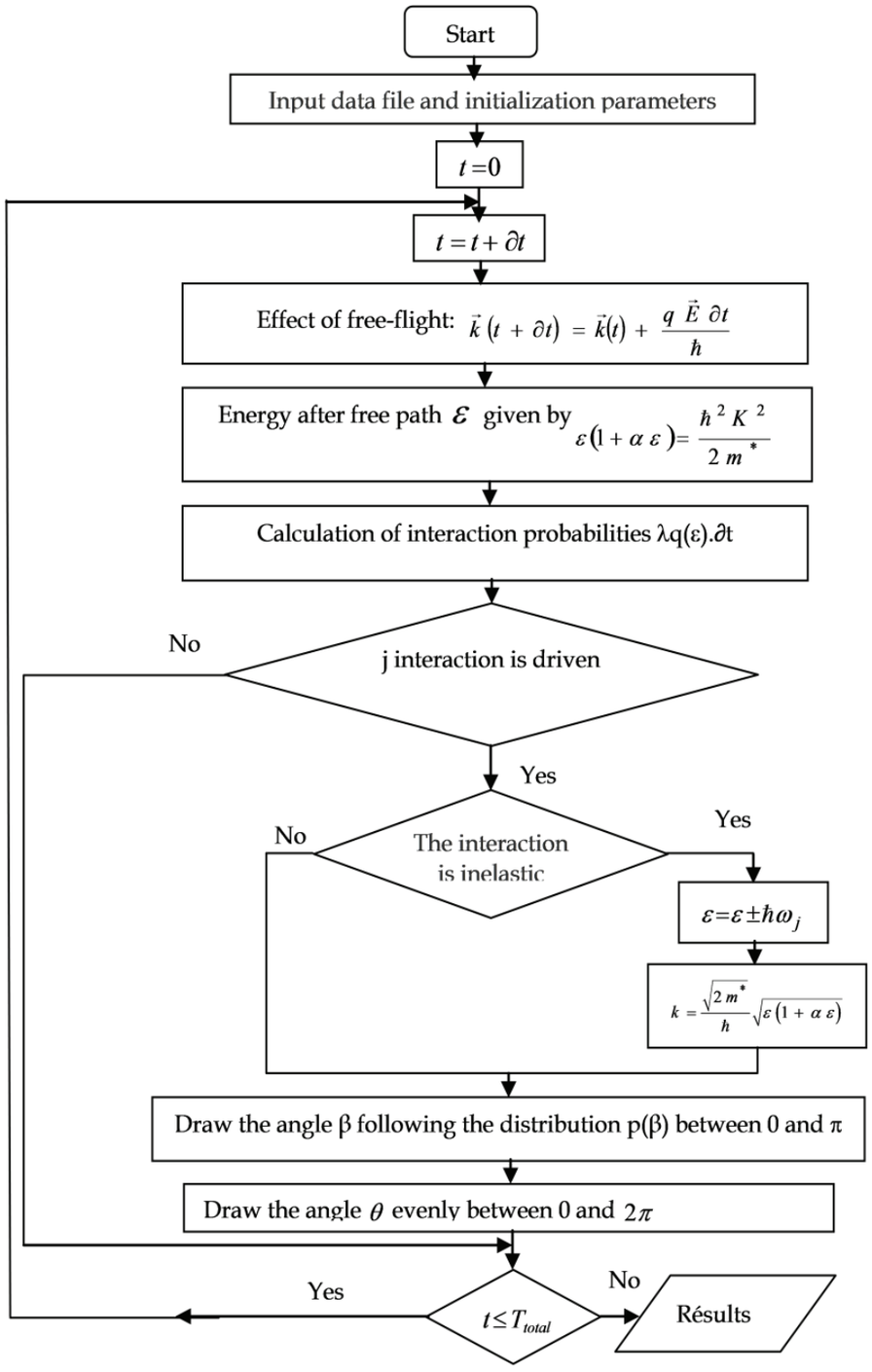

Fig. 6. Monte Carlo flowchart.

3.2 Results in the stationary regime

3.2.1 The electron energy versus the applied electric field

At room temperature and for an electron concentration of 1017cm-3, we calculate the electron energy versus the applied electric field within AlGaN and InGaN alloys, for different Al and In mole fractions. The results are illustrated by Figure 7.

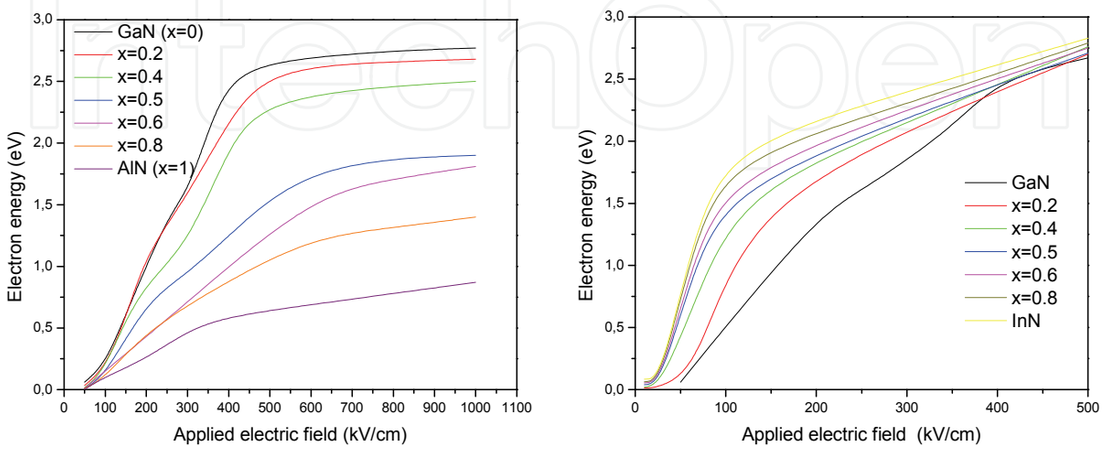

Fig. 7. The electron energy versus the applied electric field within AlGaN and InGaN alloys, for different Al and In mole fractions.

By increasing the Al mole fraction within AlGaN alloy, the energy gap increases, so it is necessary to apply an electric field harder to cross it. Therefore, the critical electric field (for which the electrons move from the valence band to the conduction band) becomes larger, it reaches 300kV/cm for AlN, and so it does not exceed 150kV/cm in GaN. In addition, the intervalley energy (E_{LX}) decreases with increasing Al mole fraction, so that the average energy decreases, it does not exceed 1eV in the case of AlN, while that of GaN is around 2.6 eV. However; within InGaN, by increasing the In mole fraction, the energy gap decreases, so the critical electric field also decreases, it is about 50kV/cm for InN. In addition, the intervalley energy becomes slightly larger and therefore the average energy increases slightly, it is around 2.85eV for InN. The energy of electrons becomes more important for electric fields relatively small compared to the AlGaN alloy.

3.2.2 Electron drift velocity versus the applied electric field

The electron drift velocity versus the applied electric field within AlGaN and InGaN alloys, at room temperature and for an electron concentration of 10^{17} cm^{-3}, is illustrated by Figure 8, for different mole fractions.

By increasing Al mole fraction within AlGaN; the energy gap, the energy between Γ and L valleys, and the electron effective mass, increase. The growth of the electron effective mass in the central valley causes decrease in its drift velocity, and displacement of the critical field to larger values of the electric field. Beyond the critical field, electrons move to the upper valley, their masses increase and they will suffer more collisions with other electrons already present in these valleys; their speed will therefore decrease.

For InGaN, increasing the In mole fraction leads to a decrease in energy gap and in effective mass of electrons in the central valley, while the effective mass of electrons in the upper valleys increases. The decrease in the effective mass of electrons in the central valley, causes an increase in their speed, and reduced energy gap results in a shift of the critical field to smaller values of the electric field. However; due to the decrease in energy between the Γ and L valleys, and the intervalley increase in collisions due to the increase of population in the satellite valleys, there is a decrease in drift velocity.

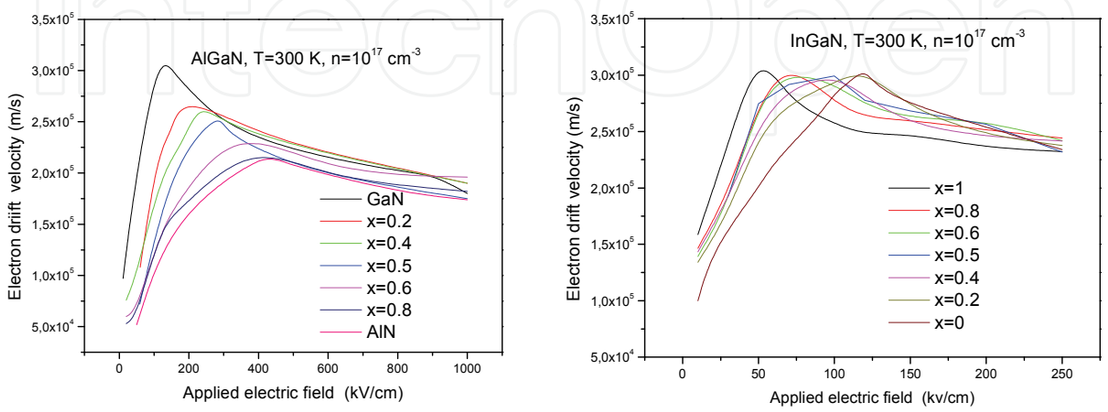

Fig. 8. The electron drift velocity within AlGaN and InGaN alloys, versus the applied electric field for different mole fractions (x = 0, 0.2, 0.4, 0.5, 0.6, 0.8, 1) at a temperature of 300K.

In conclusion, the electron velocity increases with the In mole fraction within InGaN alloy, but the electrons reach the saturation velocity for relatively small electric fields ($E \leq 500kV/cm$). Within AlGaN alloy; the electron velocity is smaller, but the electrons reach the saturation velocity for electric fields much higher ($E \geq 1000kV/cm$).

3.2.3 The electron drift velocity versus the applied electric field for different temperatures

Always for an electron concentration of 1017 cm-3 and for different mole fractions, we calculate the electron drift velocity versus the applied electric field for different temperatures: from 77K to 1000K within AlGaN and from 77K to 700K within InGaN. The results are respectively illustrated by Figures 9 and 10.

The electron velocity keeps almost the same pace. The higher velocities are reached for low temperatures; the best one is obtained for a temperature of 77K corresponding to the boiling point of nitrogen.

The increase in temperature allows a gain in kinetic energy to the electrons; they move more and collide with other atoms by transferring their energies; then their velocity decreases.

The scattering of electrons is dominated by collisions of acoustic phonons, ionized impurities, and polar optical phonons which are removed to very low temperatures, leading to improved mobility and improved velocity. At low electric field and for temperatures up to 300K, the impurities dispersion dominates and therefore there is an increase in their velocity. At high temperatures, the bump disappears due to the dominance of polar optical phonon collisions with a collision reduction of impurities.

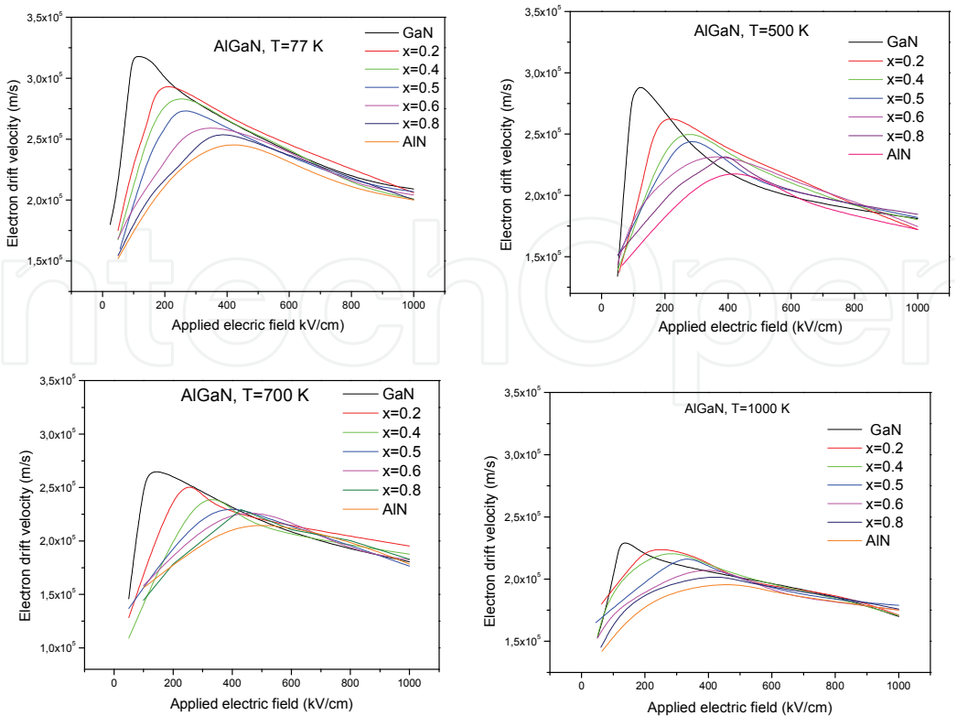

Fig. 9. The electron drift velocity versus the applied electric field within AlGaN, for different Al mole fractions at temperatures of 77K, 500K, 700K, and 1000K.

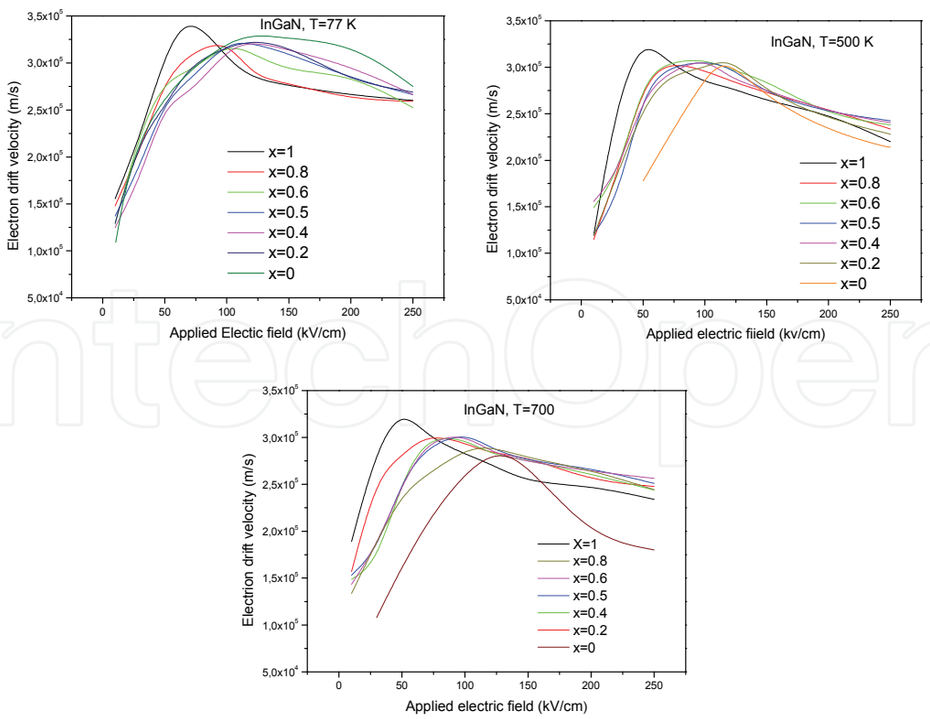

Fig. 10. The electron drift velocity versus the applied electric field within InGaN, for different In mole fractions at temperatures of 77K, 500K, and 700K.

The maximum temperature that can be applied within InGaN does not exceed 700K. Indeed, InN has a relatively small gap compared to the other nitrides, and thus even InGaN alloy has a small gap. Considering equation (1), one easily deduces that the gap becomes very small when the temperature increases.

Electron velocity is more important in InGaN for low temperatures, but the temperature can not exceed 700K. As against, the temperature can go beyond 1000K within AlGaN alloy.

3.3 The electron velocity in the transient regime

To highlight the effects of non-stationary transport that can occur in both InGaN and AlGaN alloys, we study the behavior of a bunch of electrons subject to sudden variations of the electric field, ie we apply levels of electric field.

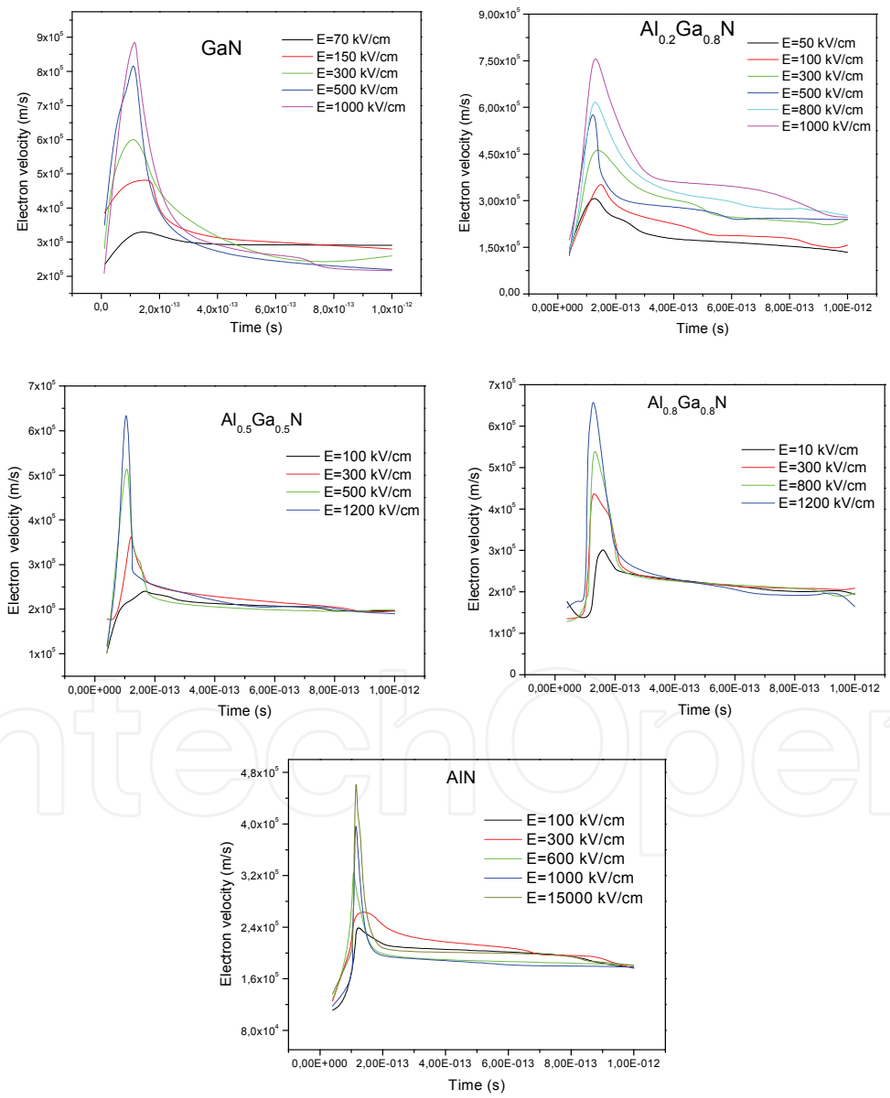

Fig. 11. The electron velocity versus the time for different levels of electric field within GaN, $Al_{0.2}Ga_{0.8}N$, $Al_{0.5}Ga_{0.5}N$, $Al_{0.8}Ga_{0.2}N$ and AlN.

To ensure a stable behavior to the electrons, we apply a field of 10kV/cm during a time equal to 1ps. Then, the electrons undergo a level of electric field. The results for AlGaN and InGaN alloys are respectively illustrated by Figures 11 and 12.

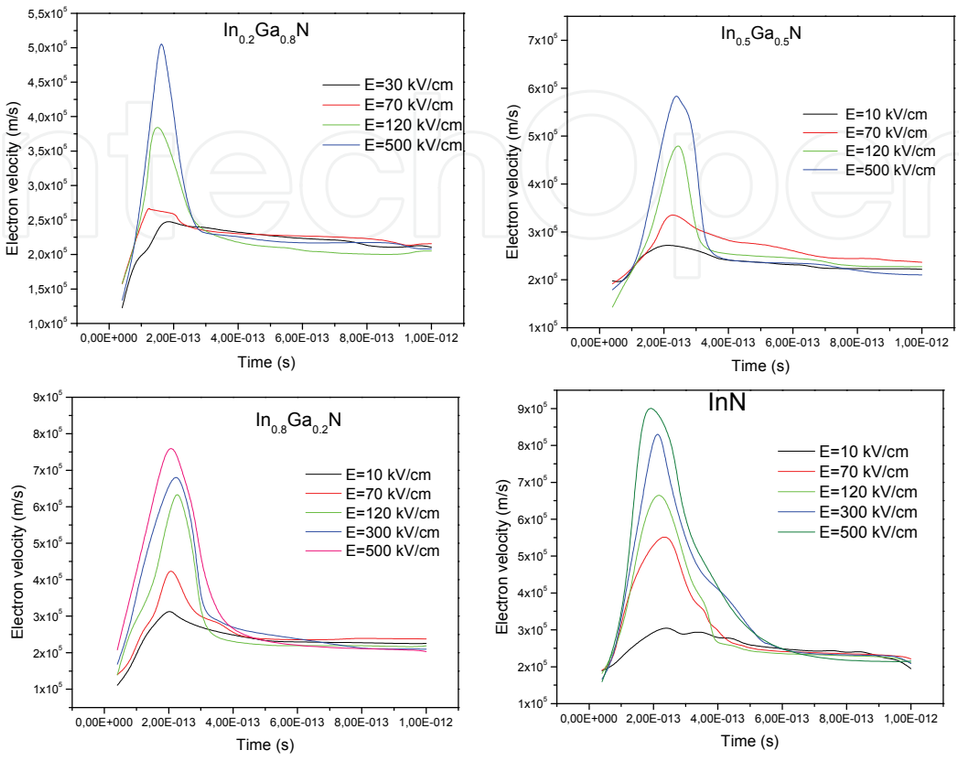

Fig. 12. The electron velocity versus the time for different levels of electric field within $In_{0.2}Ga_{0.8}N$, $In_{0.5}Ga_{0.5}N$, $In_{0.8}Ga_{0.2}N$ and InN.

Overshoots within InGaN alloy, are very large and increase with the In mole fraction. Within AlGaN alloy, they are relatively smaller and decrease with increasing the Al mole fraction.

The response time is very small in both alloys, of the order of picoseconds (see smaller); meaning that the lifetime of the electrons is very large, which is very important in optoelectronic devices.

Within InGaN, the electron energy and the electron velocity are very important for low field and low temperature. Within AlGaN, the breakdown voltage is high thanks to the large band gap, allowing high output impedance and high saturation velocity. AlGaN is more resistant to high temperatures and high pressures.

Both alloys are complementary: InGaN is more effective at low electric fields and low temperatures; AlGaN is more efficient for large electric fields and high temperatures.

LEDs based on GaN and its alloys are used in several areas: signage, automotive, display, lighting...

Among their advantages, one can mention: the low energy consumption, the high life time (100,000 hours or more), and the security (visible LEDs do not emit ultraviolet or infrared).

Laser diodes based on GaN and its alloys are used in civilian and military applications: environmental, medical, biomedical, sensing, missile guidance, etc....

4. References

Agnès P. (1999). *Caractérisation électrique et optique du nitrure de gallium hexagonal et cubique en vue de l'obtention d 'émetteurs bleus,* PhD thesis, INSA, Lyon, France.

Anceau S., (2004), *Etude des propriétés physiques des puits quantiques d'alliages quaternaires (Al,Ga,In)N pour la conception d'émetteurs ultraviolets,* PhD thesis, University of Montpellier II, France.

Anwar A.F.M., Member S., Wu S., Richard T. & Webster. (2001). Temperature dependent transport properties in GaN, AlxGa1-xN, and InxGa1-xN semiconductors, IEEE *Transactions on Electron Devices,* vol. 48, No 3, March, pp. 567–572.

Bethoux J.M., (2004), *Relaxation des contraintes dans les hétérostructures épaisses (Al,Ga)N : une piste originale pour la réalisation de diodes électroluminescentes à cavité résonante,* PhD thesis, Nice university, France.

Bougrov V., Levinshtein M.E., Rumyantsev S.L. & Zubrilov A. (2001). Properties of Advanced Semiconductor Materials GaN, AlN, InN, BN, SiC, SiGe. *Eds. Levinshtein M.E., Rumyantsev S.L., Shur M.S., John Wiley & Sons, Inc.,* New York, 1-30.

Castagné R., Duchemin J.P, Gloanie M. & Rhumelhard Ch. (1989). Circuits integers en Arsenic de Gallium, Physique, technologie et conception, *Masson edition.*

Chuang S. L. & Chang C. S. (1996). k · p method for strained wurtzite semiconductor, *Phys. Rev*. B 54, 2491.

Davydov V.Yu., Klochikhin A.A., Emtsev V.V., Kurdyukov D.A., Ivanov S.V., Vekshin V.A., Bechstedt F., Furthmüller J., Aderhold J., Graul J., Mudryi A.V., Harima H., Hashimoto A., Yamamoto A. & Haller E.E. (2002). Band Gap of Hexagonal InN and InGaN Alloys *Phys. Stat. Sol*. (b) 234, 787.

Dessene F. (1998). *Etude thermique et optimisation des transistors à effet de champ de la filière InP et de la filière GaN*, PhD thesis, University of Lille 1, France.

Dingle R., Sell D. D., Stokowski S. E. & Ilegems M. (1971). Absorption, Reflectance, and Luminescence of GaN Epitaxial Layers, *Phys. Rev*. B 4, 1211.

Enjalbert F. (2004). *Etude des hétérostructures semi-conductrices III-nitrures et application au laser UV pompé par cathode à micropointes,* PhD thesis, University of Grenoble 1, France.

Garro N., Cros A., Garcia A. & Cantarero A. (2007). Optical and vibrational properties of self-assembled GaN quantum dots, Institute of Materials Science, University of Valencia, Spain.

Helman A. (2004). *Puits et boîtes quantiques de GaN/AlN pour les applications en optoélectronique à λ≈1,55 µm,* PhD thesis, University of Orsay, Paris XI, France.

Languy F. (2007). *Caractérisation de nanocolonnes d'In(1-x)Ga(x)N en vue d'étudier l'origine de la haute conductivité de l'InN,* Faculty of University ''Notre dame de la paix", Belgique.

Martinez G. (2002). *Elaboration en épitaxie par jets moléculaires des nitrures d'éléments III en phase cubique,* PhD thesis, INSA, Lyon, France.

Nakamura S. & Fasol G. (1997). The Blue Laser Diode, *Springer* – Berlin.

Nevou L., (2008), *Emission et modulation intersousbande dans les nanost ructures de nitrures,* PhD thesis, Faculty of Sciences, Orsay, France.

O'Leary Stephen K., Brian E. Foutz, Michael S. Shur & Lester F. Eastman (2006). "Steady-State and Transient Electron Transport within the III–V Nitride Semiconductors, GaN, AlN, and InN," *A Review J Mater Sci: Mater Electron,* vol. 17, pp. 87–126

Pankov J.I., Miller E.A., & Berkeyheiser J.E. (1971). *Rca Review* 32, 383.

Pugh S. K, Dugdale D. J, Brand S. & Abram R.A. (1999). Electronic structure calculation on nitride semiconductors, *Semicond. SCI, Technol*, vol 14, pp. 23–31.

Vurgaftman I. & Meyer J. R. (2003). Band parameters for nitrogen-containing semiconductors, *J. Appl. Phys*. 94, 3675.

Vurgaftman I., Meyer J. R. & Ram-Mohan L. R. (2001). Band parameters for III–V compound semiconductors and their alloys, *J. Appl. Phys*. 89, 5815.

Zhang Y.et al. (2000). Anomalous strains in the cubic phase GaN films grown on GaAs (001) by metalorganic chemical vapour deposition, *J.Appl. Phys,* vol. 88, N° 6, pp. 3762–3764.

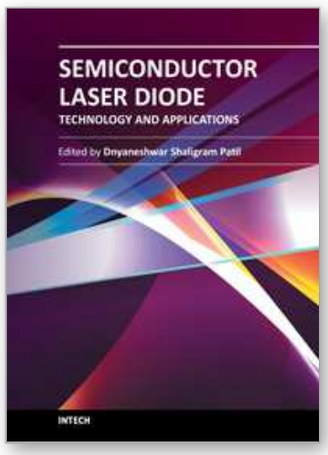

Semiconductor Laser Diode Technology and Applications

Edited by Dr. Dnyaneshwar Shaligram Patil

ISBN 978-953-51-0549-7
Hard cover, 376 pages
Publisher InTech
Published online 25, April, 2012
Published in print edition April, 2012

This book represents a unique collection of the latest developments in the rapidly developing world of semiconductor laser diode technology and applications. An international group of distinguished contributors have covered particular aspects and the book includes optimization of semiconductor laser diode parameters for fascinating applications. This collection of chapters will be of considerable interest to engineers, scientists, technologists and physicists working in research and development in the field of semiconductor laser diode, as well as to young researchers who are at the beginning of their career.

InTech Europe
University Campus STeP Ri
Slavka Krautzeka 83/A
51000 Rijeka, Croatia
Phone: +385 (51) 770 447
Fax: +385 (51) 686 166
www.intechopen.com

InTech China
Unit 405, Office Block, Hotel Equatorial Shanghai
No.65, Yan An Road (West), Shanghai, 200040, China
中国上海市延安西路65号上海国际贵都大饭店办公楼405单元
Phone: +86-21-62489820
Fax: +86-21-62489821

IntechOpen